Astron. Astrophys. 325, 881–892 (1997)

ASTRONOMY
AND
ASTROPHYSICS

Results of a search for emission-line galaxies towards nearby voids. The spatial distribution

Cristina C. Popescu[1,3], **Ulrich Hopp**[1,2], **and Hans Elsässer**[1]

[1] Max Planck Institut für Astronomie, Königstuhl 17, D-69117 Heidelberg, Germany
[2] Universitätssternwarte München, Scheiner Str.1, D-81679 München, Germany
[3] The Astronomical Institute of the Romanian Academy, Str. Cuţitul de Argint 5, 75212, Bucharest, Romania

Received 20 March 1997 / Accepted 16 April 1997

Abstract. We present the results of a search for emission-line galaxies (ELGs) towards nearby voids, based on a sample selected on the HQS (Hamburg Quasar Survey)(Hagen et al. 1995) - III-aJ objective-prism plates. The survey was based on the presence of emission-lines and therefore has the advantage to detect very faint objects (with all the flux in the emission-lines and almost no continuum), that would be missed by an apparent magnitude limited survey. We found objects as faint as B=20.5 and $M_B = (-15.0, -12.0)$. The relevant brightness parameters of the sample are: (1) the sum of the flux in the emission-lines and of the continuum flux under the line, and (2) the equivalent widths (EW); the corresponding completeness limits are 6.7×10^{-14} erg sec^{-1}cm^{-2} and 8 Å, respectively.

The observational data are given in Popescu et al. (1996) and in the present paper we consider a complete subsample from these data. We analyse the spatial distribution of our sample of ELGs in comparison with the distribution of normal galaxies. Overall both distributions trace the same structures. Nevertheless we also found a few ELGs in voids, from which at least 8 lie in the very well defined nearby voids. The isolated galaxies seem to form fainter structures that devide the larger voids into smaller ones. From our estimates of the expected number of void galaxies we conclude that we did not find an underlying homogenous void population.

Key words: large scale structure – galaxies – redshift survey – galaxies: clusters – galaxies: compact

1. Introduction

The large scale structure of the Universe, as derived from recent redshift surveys, reveals us large inhomogeneities: we see the galaxies forming clusters and superclusters, or even larger structures, filaments and sheets of galaxies, or walls, which surround the empty regions that are the voids. But this view is primary based on the high luminosity galaxies - the giants. There has been a long debate in the literature whether the giant galaxies are fair tracers of the large scale structure and whether the voids are really empty. From an observer point of view, the galaxy maps may reflect special observational selection effects in surface brightness, integral magnitude or diameter. It is a straightforward idea to think that going fainter we will eventually start to fill the voids. We know that the dwarf galaxies dominate the galaxy number in the Universe, but only very few are contained in the present galaxy catalogues. These objects can be very small, intrinsically faint and can also have very low surface brightness. The dwarf galaxies are thus good candidates to fill up the voids. There are also some theories of galaxy formation (Dekel & Silk 1986) that were worked out in the frame of the cold dark matter (CDM) scenarios including biasing, which predict that the dwarf galaxies should originate from the 1 σ fluctuations, expecting thus to be more evenly distributed than the high rare density peaks which form the giants. In these scenarios the dwarf galaxies should trace the underlying dark matter and are expected to fill the voids. It is therefore a fundamental task to search for the existence of a homogenous void population. Whether or not such a population exists would be of extreme importance for our understanding of galaxy formation and large scale structure formation and evolution.

Several studies of the spatial distribution of dwarf galaxies were carried out to answer these questions. Different projects were conceived to search for galaxies in voids or to see if the clustering properties of dwarfs galaxies are different from that of the normal giant galaxies. Most of the studies were based on redshift surveys of low-surface brightness dwarfs (Bothun et al. 1986, Thuan, Gott & Schneider 1987, Eder et al. 1989, Salzer, Hanson & Gavazzi 1990, Binggeli, Tarenghi & Sandage 1990, Weinberg et al. 1991, Thuan et al. 1991). The results of these studies did in general not favour biased galaxy formation and no void population was found. More recently, a new search for faint galaxies in voids was accomplished, with the intention to overcome the limitations of previous surveys in magnitude,

Send offprint requests to: Cristina C. Popescu

diameter and surface brightness (Hopp 1994, Hopp et al. 1995, Kuhn et al. 1997). Other studies were based on emission-line objects (Tifft et al. 1986, Moody et al. 1987, Weistrop & Downs 1988, Weistrop 1989, Salzer 1989, Rosenberg et al. 1994) and there has been the suggestion that a few emission-line galaxies have been found in the voids. Much effort has concentrated on the study of the Bootes void, a huge low density region with a volume of $1.3 \times 10^5\,\mathrm{Mpc}^3$, first discovered by Kirshner et al. (1981) (see also Kirshner et al. 1983 a,b). Up to now 58 galaxies were identified in the Bootes void, most of them coming from objective-prism surveys (Sanduleak & Pesch 1982, Tifft et al. 1986) but also from IRAS (Dey et al. 1990) and HI surveys (Szomoru et al. 1996a). The studies of the properties of these galaxies (Weistrop et al. 1995, Szomoru et al. 1996b) showed that they were strong emission-line objects with significant amount of star formation. They were also luminous galaxies, not the low mass, low surface brightness galaxies predicted to be found in voids. On the other hand it is important to notice that the Bootes void is beyond the distance at which the large scale structure is well defined by the present catalogues.

Having in mind that no definitive conclusion was drawn from previous studies and no faint void population was found in literature, we have undertaken a programm to search for dwarf galaxies in voids (Popescu et al. 1995, Popescu 1996). We especially selected nearby voids which were very well defined in the distribution of normal galaxies, in order to overcome some of the limitations of previous surveys like those in Bootes. Since there was a hint that emission-line galaxies were found in voids, we chose to search for emission-line objects, but with the aim of finding mainly dwarf HII galaxies or BCDs. The observational data of our survey as well as the location of our void regions are given in Popescu et al. (1996) (Paper 1). The candidates were selected on the objective prism plates taken from the Hamburg Quasar Survey (HQS)(Hagen et al. 1995) and therefore they have the name built with the prefix HS.

In this paper we will give the results of our search for galaxies in voids and we will describe the spatial distribution of the ELGs in comparison with the normal galaxies. The paper is organised as follows. In section 2 we estimate the completeness of our survey in terms of fluxes and equivalent widths. In section 3 we give a qualitative description of the spatial distribution of our ELGs, by using cone-diagrams in both Right-Ascension and Declination projection, and we also quantify the results by calculating the spatial densities and the nearest neighbour distributions. In section 4 we analyse the main properties of the galaxies we found in voids and in the last section we summarise and give the conclusions.

2. The completeness of the survey

In Paper 1 we have discussed in detail the selection of our sample and the selection effects. In summary, an automated procedure was applied to the low-resolution digitised objective-prism spectra, based on two parameters, the slope of the continuum and the "luminosity"of the integrated spectra (in counts). The selected candidates were afterwards rescanned with high resolution and the final selected spectra were visually inspected for the presence of emission-lines. While the slope of the continuum helps us to preselect very promising emission-line candidates, the cut in brightness at the faint end of the photographic plates produces some loss of very faint objects, with very little continuum and almost all the flux in the emission-lines. In order to prevent the latter incompleteness we also scanned the faint end of the photographic plates, and we completed the follow-up spectroscopy for all the faint candidates. This extra survey was done only for one of our regions - Region 3 from Paper 1 (a region North to the Coma Supercluster, $30.5^\circ < \delta < 45.5^\circ$, centred around 13.5^h) and in the following discussion we will refer only to this subsample. The surface density of the subsample is 0.3 galaxies/deg^2 and the catalogue of the additional survey will be published elsewhere. For the data analysed in this paper we have completed the spectrophotometry, allowing thus to establish a completeness limit. Our sample was not selected in a traditional way, therefore it is not a continuum magnitude limited sample. Nevertheless we can first give the limits of our survey in continuum blue magnitudes, based on the data from Paper 1 and from the additional survey. Our sample contains objects as faint as $\mathrm{B}_{lim} = 20.5$, and also intrinsically faint objects, down to $\mathrm{M}_B = (-15.0, -12.0)$. This indicates that the present survey goes deeper than other surveys and is therefore adequate for a search for faint objects in voids. But for a sample that was selected based on the presence of the emission-lines, the relevant brightness parameters are the sum of the flux in the emission-lines and of the flux in the continuum under the line, and the equivalent widths. A detailed description of this selection procedure is given by Salzer (1989).

As the main selection was based on the presence of the [OIII] λ5007 line, the corresponding parameters for this line were computed. A complete catalogue with fluxes and equivalent widths (EW) will be published in a following paper. All the spectroscopic parameters calculated here are $4''$ slit widths measurements. The line flux F_L was measured directly from the slit spectra. The flux in the continuum under the line was calculated as $\mathrm{F}_C = \mathrm{f}_c\,\Delta\lambda$, where f_c is the mean flux per unit of wavelength and $\Delta\lambda$ is the FW0I (flux width at zero intensity) of the emission-line. f_c is calculated as the ratio between the line flux and the EW of the line, $\mathrm{f}_c = \mathrm{F}_L/\mathrm{EW}$ and it can be measured directly from the slit spectra.

$\Delta\lambda = 2\,\mathrm{Disp(z)R}$, where Disp(z) is the reciprocal dispersion of the objective prism in Å mm^{-1} and R is the spectral resolution on the objective prism plates. In our case the resolution R is determined by the slit widths of the PDS machine that was used to digitise the plates. For the high resolution scans (see Paper 1 for further details) we used a slit of 0.03 mm and we can assume that this is also the value of R[1]. The resulting $\mathrm{F}_{L+C} = \mathrm{F}_L + \mathrm{F}_C$ as well as the EW of the [OIII] λ5007 lines were computed for each individual object of our sample. For two cases the H_β was

[1] Because we selected only high quality plates, the broadening of the lines by seeing is almost negligible compared to the PDS slit width, as 0.03 mm corresponds to about $2''$.

Table 1. The V/V$_m$ test.

m$_{L+C}$ (1)	V/V$_m$ (2)	N (3)	N′ (4)	c% (5)
10.8	0.581	12	0	100.0
10.9	0.597	16	0	100.0
11.0	0.575	19	0	100.0
11.1	0.536	21	0	100.0
11.2	0.502	23	0	100.0
11.3	0.527	29	0	100.0
11.4	0.473	30	2	93.3
11.5	0.477	35	1	92.1
11.6	0.452	38	3	86.4
11.7	0.459	44	2	84.6
11.8	0.464	51	1	85.0
11.9	0.453	57	4	81.4
12.0	0.433	62	6	76.5
12.1	0.414	67	8	71.2
12.2	0.389	71	11	65.1
12.3	0.368	75	13	59.5
12.4	0.334	77	17	53.1
12.5	0.327	82	17	49.1
12.6	0.324	88	20	45.6
12.7	0.283	88	29	39.6
12.8	0.273	92	30	35.9
12.9	0.258	95	35	32.3
13.0	0.225	95	44	28.1
13.1	0.203	96	50	24.7
13.2	0.184	97	57	21.7
13.3	0.167	98	66	19.1
13.4	0.146	98	76	16.6
13.5	0.134	99	87	14.6

stronger than the [OIII] lines, indicating starburst like galaxies, and therefore Hβ was measured instead.

The F$_{L+C}$ was transformed in a magnitude scale:

$$\mathrm{m}_{L+C} = -2.5 \times log10(\mathrm{F}_{L+C}) - 20.9, \quad (1)$$

where the constant is arbitrary.

Our sample contains objects with the flux of the [OIII] λ5007 emission-line as faint as 5.3×10^{-15} erg sec^{-1} cm^{-2} and as bright as 5.3×10^{-13} erg sec^{-1} cm^{-2}. If we consider the brightness parameter discussed above, namely the sum of the flux in the emission-line and of the continuum under the line, then the range is 9.5×10^{-15}erg sec^{-1} cm^{-2} $<$ F$_{L+C}$ $<$ 8.0×10^{-13}erg sec^{-1} cm^{-2}. The EW values range between 8 Å and 1700 Å.

The completeness limit was derived based on a V/V$_m$ test (Schmidt 1968). V is the volume contained in a sphere whose radius is the (redshift) distance to the object and V$_m$ is the volume contained in a sphere whose radius is the maximum distance the galaxy could have and still be in the sample under study,

$$\mathrm{V}_m = \frac{4}{3}\pi \times 10^{0.6(\mathrm{m}_{lim}-\mathrm{M}-\mathrm{A}-25.0)} \quad (2)$$

where m$_{lim}$ is the completeness limit and A is the Galactic absorption.

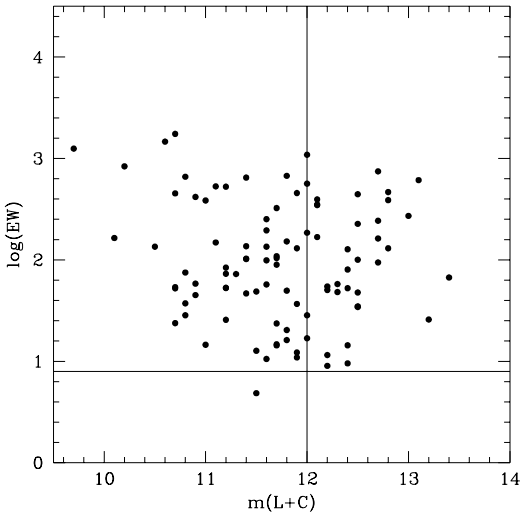

Fig. 1. A plot of log(EW) versus m$_{L+C}$, where EW are the equivalent widths in Å and m$_{L+C}$ is the flux in the emission-line plus the flux in the continuum under the line, transformed in a magnitude scale (see (1)). With the vertical line we delimit the complete sample from the incomplete one and with the horizontal line we trace the threshold below which the ELGs are no more seen by our survey.

The value of V/V$_m$ is then given by $10^{0.6(m-m_{lim})}$. The mean value of the ratio V/V$_m$ should be 0.5 for a complete sample of objects uniformly distributed in Euclidian space. In practice the distribution of galaxies is affected by large scale structure inhomogeneities. As a first approximation we can consider that our subsample covers enough volume (415 deg^2, v$\leq$ 15000 km/s) to cancel out these effects. Also we will show that the ELGs have a small tendency to be more evenly distributed than the giant galaxies, lying also in some voids or at the rim of the voids, and therefore the approximation of uniformity can be applied as a first guess.

The mean V/V$_m$ ratios were computed for 99 galaxies in our Region 3 and the results are listed in Table 1. The Column (1) gives the m$_{L+C}$, Column (2) gives the V/V$_m$ ratios and Column (3) gives the total number of objects brighter than the corresponding m$_{L+C}$. Column (4) specifies the number of objects that need to be added at each level of magnitude in order to keep the average V/V$_m$ around 0.5 and Column (5) gives the level of completeness, c%. The V/V$_m$ ratios are around 0.5 up to m$_{L+C}$ = 11.4 and then they start to decrease. We will take as a completeness limit m$_{L+C}$ = 12.0, where the sample is 77% complete. This corresponds to a flux of 6.7×10^{-14}erg sec^{-1}cm^{-2}.

In order to determine also the EW limit of our survey we plotted in Figure 1 log(EW) versus m$_{L+C}$. With the vertical line we delimit the complete sample from the incomplete one and with the horizontal line we trace the threshold below which the ELGs are no more seen by our survey. This is a level of 0.9, which means an EW = 8Å. There is only one point that falls below the horizontal threshold of 0.9. The corresponding galaxy was selected based on its [OII] λ3727 line, one of the few cases that did not use only the [OIII] λ5007 line criteria. Its

spectrum is typical for a low ionization object, with faint [OIII] λ5007 and strong [OII] λ3727 emission lines. If one computed the EW for the [OII] λ3727 line, the galaxy would fall above the horizontal threshold. One should also mention that all the points that were just above this threshold were galaxies selected as second priority objects (see Paper 1 for a detailed discussion of the selection procedure). The corresponding emission-lines were barely detectable on the digitised spectra, and we had difficulties to decide whether the candidate was real or not. The follow-up spectroscopy was the only method to determine the real nature of the objects. Therefore, removing these points from the plot, the diagram would indicate a slightly higher limit in EW, toward 12 Å.

The diagram also shows a trend of increasing EW at both the bright and the faint end of the m_{L+C}. At the very bright end the galaxies have a strong continuum, and therefore it requires a higher EW for the emission-line to be detected above the continuum. By contrary, at the faint end, the galaxies have a low level continuum and therefore the spectrum is quite noisy. It requires again a high EW for the emission-line to be detected above the noise. In addition the sum between the flux in the emission-line and the continuum flux has to be kept above a certain level of detectability, and as the continuum decreases, the flux in the emission-line has to increase in order to detect the galaxy.

In conclusion we can build a complete sample with all the objects brighter than $F_{L+C} \geq 6.7 \times 10^{-14}$erg sec^{-1}cm^{-2} and having a detectability in equivalent widths EW$\geq$ 8Å. Such a sample cannot be compared with a magnitude selected sample, but can be used for statistical calculations.

3. The distribution of ELGs

3.1. The space densities

We calculate the space densities of our sample of ELGs using a V/V_m method applied to the parameter m_{L+C}, as defined in the previous section. Through this paper we used a Hubble constant H_0 = 75 km/s/Mpc. We computed a corresponding "absolute magnitude", which is the intrinsic flux of the emission-lines plus the continuum under the line, transformed in a magnitude scale, M_{L+C}. We should once again mention that these so called absolute magnitudes do not have the meaning of the continuum absolute magnitudes and should be interpreted as the intrinsic strength of the emission-lines. The space density at M_{L+C} is:

$$\Phi(M_{L+C}) = \frac{4\,\pi}{\Omega} \sum_i (\frac{1}{V_m^i}) \quad \mathrm{Mpc}^{-3}\,\mathrm{mag}^{-1} \tag{3}$$

where Ω is the solid angle covered by our survey, and the summation is over all galaxies in the absolute magnitude interval $M_{L+C}\pm0.5$ mag. The absolute magnitudes were calculated considering a Galactic absorption given by $A = 0.23/(sin|b|)$.

In the computation of the $\Phi(M_{L+C})$ we included all galaxies up to a m_{L+C} = 12.5, for which the completeness level is 49.1%. Thus we must increase the calculated space densities by a factor of 2.04 to allow for incompleteness. In Table 2 we listed the $log\Phi(M_{L+C})$ for each bin of absolute magnitude together with the number of galaxies included in each bin.

Table 2. Space Densities $\Phi(M_{L+C})$.

M_{L+C} (1)	$log\Phi(M_{L+C})$ (2)	N (3)
-27.0	-6.34	2
-26.0	-5.72	3
-25.0	-4.40	17
-24.0	-3.78	18
-23.0	-3.13	21
-22.0	-2.86	9
-21.0	-2.48	6
-20.0	-2.27	3
-19.0	-1.46	3

Table 2 shows that we found only a few extreme strong [OIII] λ5007 line objects (5%) and that most of our objects (57%) have high and intermediate strengths of the emission-lines. Going to objects that have intrinsically faint [OIII] λ5007 lines, our survey becomes less efficient, and some of these objects can be better detected by Hα surveys (see Zamorano et al. 1994).

The integration over the whole range of absolute magnitudes M_{L+C} gives a space density of $0.046\pm0.005\,\mathrm{Mpc}^{-3}$. In order to calculate the corresponding error we considered different completeness limits and we estimated the spread around the assigned value. The integrated space density is nevertheless dominated by the last bin (at the faint end) of the luminosity function, which was calculated based only on three galaxies. This point is therefore very uncertain and we prefer to give a space density integrated only till $M_{L+C} = -20.0$. Then we obtain $\Phi = 0.011 \pm 0.001\,\mathrm{Mpc}^{-3}$, which is a factor 3.5 lower then the previous value. The results for different completeness limits are now more stable, with the estimated error a factor 5 lower.

3.2. Cone-diagrams

A study of the spatial distribution of the ELGs requires a comparison with a catalogue of normal galaxies that would properly trace the main structures in the nearby Universe and would also properly define the nearby voids. We have already mentioned in the introduction that we selected our surveyed regions to contain well defined nearby voids in the distribution of the giant galaxies. For the comparison catalogue we used the latest electronic version of the ZCAT (April 1995)[2] and we selected all galaxies brighter than B=15.5. The ZCAT contains only one strip that is complete to 15.5^m. This is the so called "Slice of the Universe", $26.5^\circ < \delta < 32.5^\circ$ and $8^h < \alpha < 17^h$. Our surveyed regions are outside the zone of the Slice, therefore the catalogue is not complete to 15.5^m. The incompleteness of the comparison catalogue do not affect the qualitative description of the large-scale structure, as given by the cone-diagrams, but

[2] For the description of the catalogue see also Huchra et al. 1992, Huchra et al. 1995.

could affect the results of some statistical tests, as mentioned in the next section.

The most common way to visualise the spatial distribution of galaxies is to use cone diagrams in both redshift-Right Ascension and in redshift-Declination plane. Since we give a qualitative description of the spatial distribution, we have plotted all ELGs, without respect to their completeness. Such a restriction is done only when we apply statistical tests (see subsection 3.3). The diagrams contain also the comparison catalogue (the ZCAT galaxies brighter than 15.5). In addition we have plotted the ZCAT galaxies fainter than 15.5, with the intention to have a first impression of how the fainter galaxies start to structure and how they correlate with the ELGs. In the following description we will use the term bright ZCAT for the ZCAT galaxies with apparent magnitudes brighter than B=15.5 and the term faint ZCAT for the ZCAT galaxies fainter than B=15.5. The terms bright and faint do not therefore refer to the intrinsic brightness of the comparison galaxies. As most of our galaxies are fainter than 15.5, there is practically no overlap in apparent magnitudes between our sample and the comparison (bright) catalogue.

All velocities are corrected for the Galaxy's motion with respect to the velocity centroid of the Local Group. We use a correction term of Δv = 300 sin(l) cos(b) (Sandage 1975), where l and b are the galactic coordinates. We plotted all the galaxies with velocities out to 15000 km/s, which corresponds to a redshift of z = 0.05, including thus most of our sample. For velocities greater than 15000 km/s the comparison catalogue becomes essentially non-existent. Already for velocities greater than 10000 km/s the ZCAT quickly thins out, and therefore we refrain from drawing conclusions about the reality of voids beyond 10000 km/s.

In the cases where our surveyed region was too narrow in one dimension or not properly covering some main features of the large scale structures, a bigger area of sky is displayed. In these cones the surveyed region is either delimited with dotted lines or some specifications are given in the Captions. We should also mention that our cone diagrams do not completely cover all the surveyed region, and the strips are chosen to display the most relevant information. The cones plotted in Fig. 2 a,b contain a larger angle in Right Ascension than our surveyed region, because we did not want to cut through the very well defined foreground voids and we wanted to have a better impression of the large scale structure in this region. The actual surveyed region is only between $12^{\rm h}$ and $15^{\rm h}30^{\rm m}$.

The strip plotted in Fig. 2 a is slightly to the North of the "Slice of the Universe". For this reason we can still see some of the prominent features of the Slice, remnants of the "Harvard Sticky Man" at velocities less than 7500 km/s, but without the Coma Cluster. The most remarkable feature of the diagram is the "Great Wall", which crosses our diagram from 6500 km/s at $\alpha = 12^{\rm h}00^{\rm m}$ to 9000 km/s at $\alpha = 15^{\rm h}30^{\rm m}$. The structures of the Sticky Man define some foreground voids, of which that centred at $\alpha \sim 13^{\rm h}15^{\rm m}$, v $\sim$ 3000 km/s is one of the best defined void in our surveyed region and we will call it Void 1. In the front of the Great Wall there is a very big void that opens to the western side of the cone and continues also outside our actual survey. We will call it Void 2. Void 1 and Void 2 will be used to draw our conclusions about the void population. Beyond the Great Wall there is another big void, but the size of the void is no more well defined by the ZCAT galaxies because at these distances the comparison catalogue becomes practically non-existent.

Our galaxies seem to follow the structures described above as well. At a closer inspection one can discover that there are some galaxies that lie very isolated in some of the foreground voids. In Void 1 there are two galaxies, HS1236+3821, v = 2215 km/s and HS1226+3719, v = 3306 km/s, that have the nearest bright ZCAT galaxy at a distance of 3.85 h^{-1} Mpc and 6.63 h^{-1} Mpc, respectively (for detailed description of the isolated galaxies see Table 3). At this distance the mean separations between galaxies is around 0.5 h^{-1} Mpc, so these two galaxies are extremely isolated. They are among the best candidates we found in the voids. Two further faint ZCAT galaxies are also present in the void (see Table 4). In Void 2 we found an "Arch"of 7 ELGs (HS1236+3937, HS1232+3947, HS1240+3721, HS1332+3426, HS1328+3424, HS1310+3801), that seem to divide the void into three smaller voids. The galaxy HS1236+3937 has the largest isolation, of 8.68 h^{-1} Mpc. The Arch is also populated by three faint ZCAT galaxies while a fourth one closes the Arch at lower redshifts (Table 4). In the background void beyond the Great Wall there are two HS galaxies, one at 8131 km/s, HS1306+3320, and one at v = 9558 km/s, HS1410+3446. However we have already mentioned that this background void is not delimited at the far distance edge by the bright ZCAT galaxies, but mainly by our ELGs and by some faint ZCAT galaxies. It is anyway remarkable the large number of ELGs we found at higher redshifts, where the ZCAT catalogue do not contains any galaxy.

Fig. 2 b displays the same region in Right Ascension but shifted to the North and having an overlap with the previous diagram of 2° in Declination. We chose a small overlap in order to see how the structures evolve when moving in one coordinate. The diagram no longer resemble the Slice, though one can still see some features of the Great Wall. There is an extra feature that appears at 6000 km/s, a filament that stretches from $\alpha = 13^{\rm h}45^{\rm m}$ up to $\alpha = 15^{\rm h}40^{\rm m}$. The two voids in the front of the Great Wall seem to converge now in a unique void centred on $\sim$ 4000 km/s. The void still contains some galaxies from the Arch, but one can see now a chain of faint ZCAT galaxies that seem to associate with the ELGs and again divide the big void in two smaller voids. The region beyond v = 12500 km/s and east to $13^{\rm h}30^{\rm m}$ contains the southwest boundary of the Bootes void (centred on $\alpha = 14^{\rm h}50^{\rm m}$, $\delta = 46°$, v = 15500 km/s) (Kirshner et al. 1981).

In Fig. 3 a we plotted in a redshift-Declination diagram the galaxies from $12^{\rm h}15^{\rm m} < \alpha < 13^{\rm h}00^{\rm m}$, the strip being chosen to cut through Void 1 and Void 2 (Fig. 2 a), containing thus some of the void galaxies. The "finger of God" that is the Coma Cluster is in fact at the border of the surveyed region, lying mainly outside it.

Fig. 3 b contains the next strip between $13^{\rm h}00^{\rm m} < \alpha < 13^{\rm h}45^{\rm m}$, plotted again in a redshift-Declination diagram. The cone contains now the easter side of the Arch and cuts through

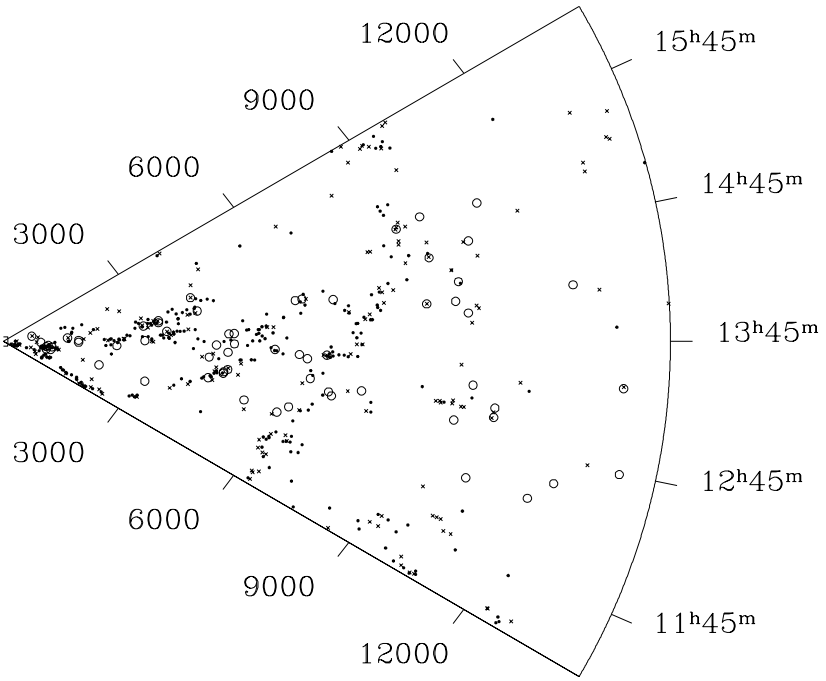

a) $33°00' < \delta < 40°00'$
· ZCAT: $m < 15.5$: N = 276
× ZCAT: $m > 15.5$: N = 165
○ HS: N = 63

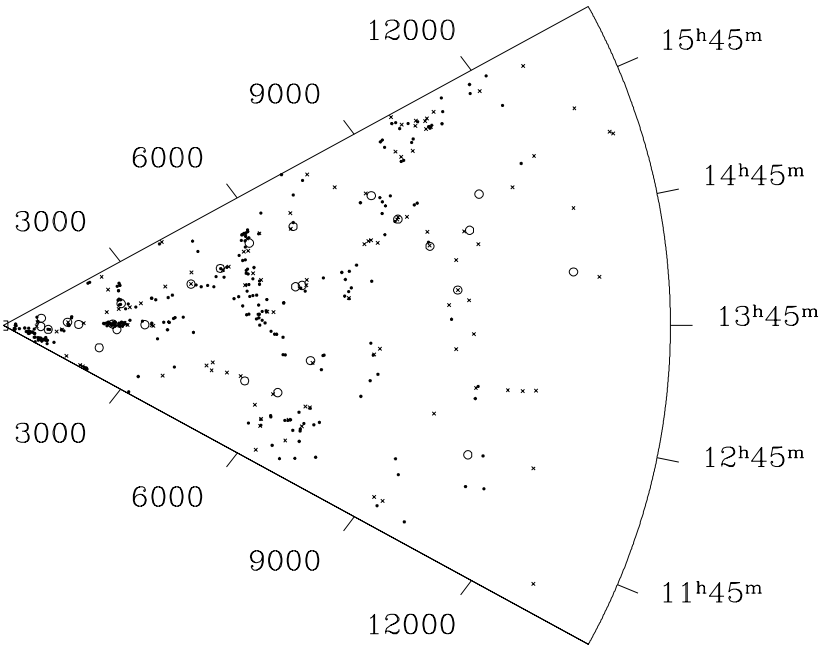

b) $33°00' < \delta < 40°00'$
· ZCAT: $m < 15.5$: N = 275
× ZCAT: $m > 15.5$: N = 115
○ HS: N = 27

Fig. 2a and b. Wedge-plots of redshift (cz in km/s) - right Ascension out to a redshift of 15000 km/s. The ZCAT $m < 15.5$: small dots, the ZCAT $m > 15.5$: crosses, the ELGs: open circles. The wedge is a 7° wide strip in Declination centred in **a)** δ = 36°30′, **b)** δ = 41°30′. The cones contain a larger angle in right Ascension than our surveyed region, which is only between (12^h, 15^h30^m).

the filaments that we mentioned as remnants of the "Harvard Sticky Man".

In Fig. 3 c we plotted one more redshift-Declination cone, for the strip in Right-Ascension $13^h45^m < \alpha < 14^h15^m$. The strip was chosen to cut through the filaments that runs in radial direction in our Fig. 2 a and therefore do not contain relevant nearby voids for our surveyed region.

In order to have a better impression of the whole surveyed region, we projected in a redshift-Right Ascension diagram (Fig. 4) a strip of 15° in Declination, from $30°30' < \delta < 45°30'$. Projection effects would of course affect the cone but in this case we are interested only to which extent the voids are still defined in the diagram. Due to the crowding of the diagram we refrain from plotting the faint ZCAT galaxies, and we consider only the comparison catalogue (bright ZCAT galaxies). It is remarkable to see that despite the large strip in Declination that was projected in the cone, the two isolated galaxies in Void 1 are still clearly isolated and the void is still very well defined. This indicates that the void extends at least 15 degrees in Declination.

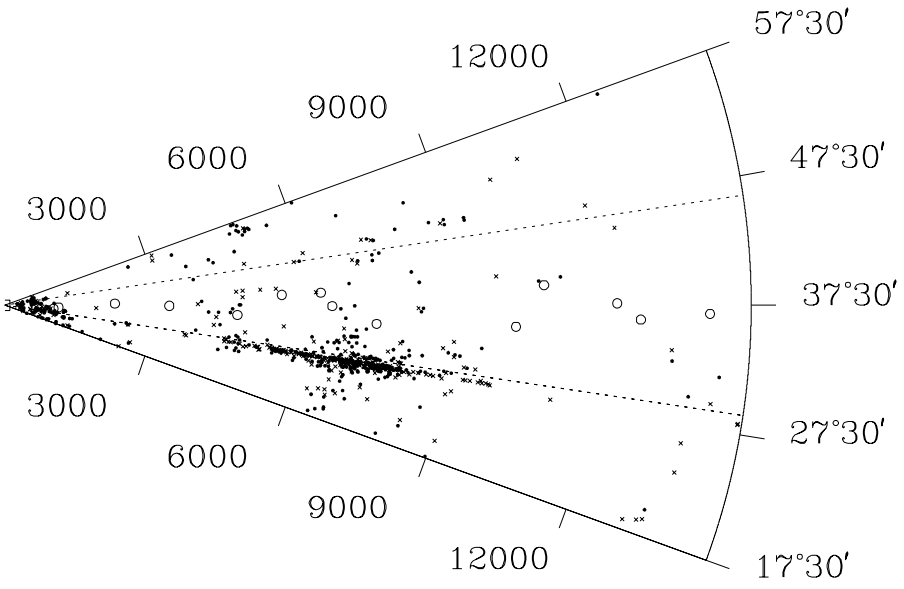

a) $12^h15^m < \alpha < 13^h00^m$
· ZCAT: $m < 15.5$: N = 349
× ZCAT: $m > 15.5$: N = 286
○ HS: N = 14

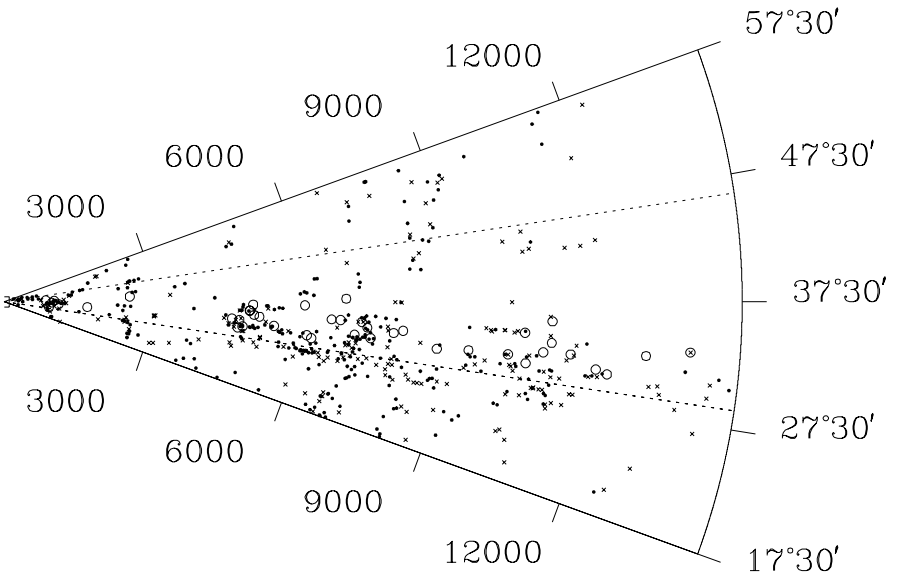

b) $13^h00^m < \alpha < 13^h45^m$
· ZCAT: $m < 15.5$: N = 286
× ZCAT: $m > 15.5$: N = 182
○ HS: N = 42

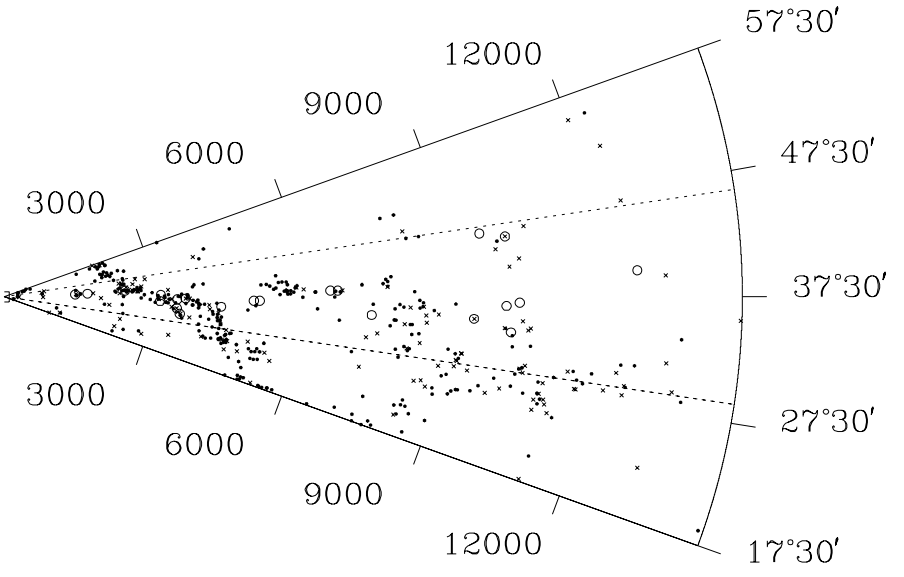

c) $13^h45^m < \alpha < 14^h15^m$
· ZCAT: $m < 15.5$: N = 297
× ZCAT: $m > 15.5$: N = 118
○ HS: N = 22

Fig. 3a–c. Wedge-plots of redshift (cz in km/s) - Declination out to a redshift of 15000 km/s. The ZCAT $m < 15.5$: small dots, the ZCAT $m > 15.5$: crosses, the ELGs: open circles. The wedge is a 45^m wide strip in Right Ascension.

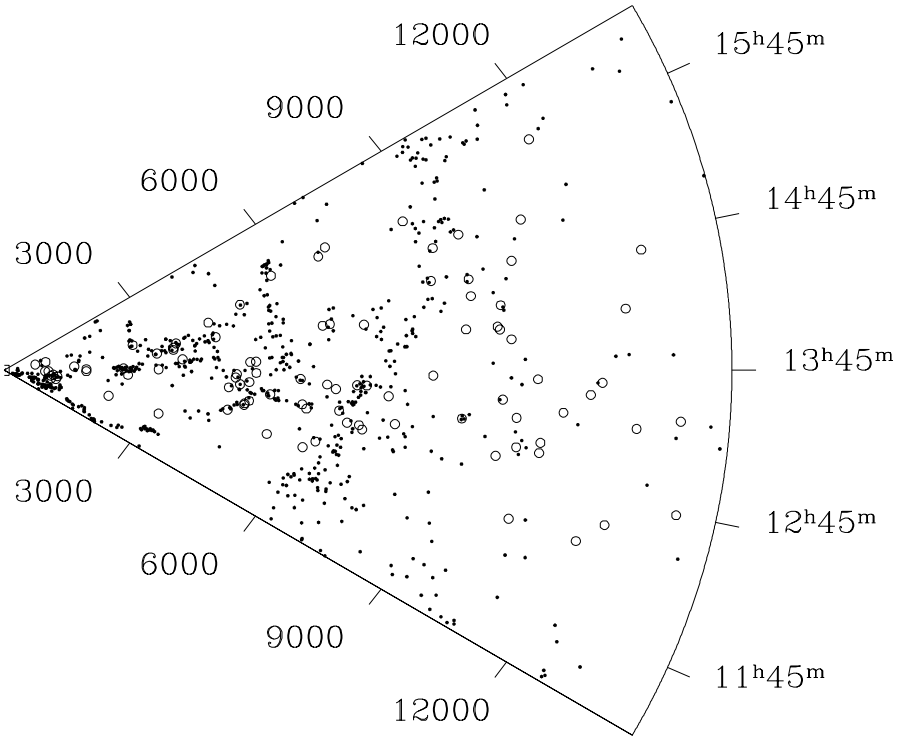

Fig. 4. Wedge-plots of redshift (cz in km/s) - Right-Ascension out to a redshift of 15000 km/s. The ZCAT $m < 15.5$: small dots, the ZCAT $m > 15.5$: crosses, the ELGs: open circles. The wedge is a 15° wide strip in Declination.

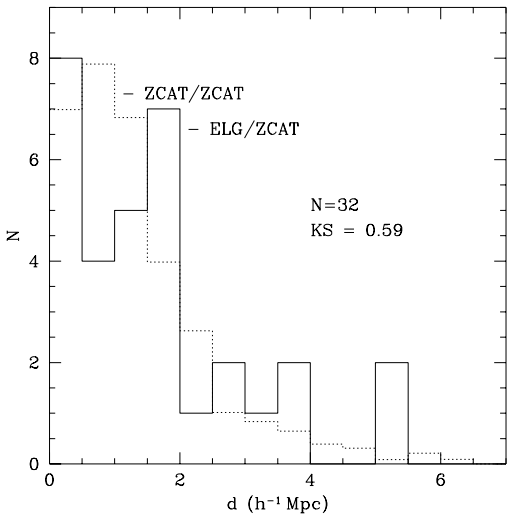

Fig. 5. The nearest neighbour distributions. The ELG/ZCAT separations are plotted with solid line and the comparison ZCAT/ZCAT distribution with dashed lines.

Overall the wedge diagrams show that our ELGs follow the structures traced by the normal galaxies. However 17 ELGs (17%) are very isolated, of which at least 8 (8%) lie in some foreground voids. There are also some ELGs that lie at the rim of the voids and there seem to be a tendency for the ELGs to be more evenly distributed that the ZCAT galaxies.

3.3. The nearest neighbour test

In order to quantify the visual impression provided by Figures 2-4, we applied some statistical tests for differences in the distribution of HS and ZCAT samples. For the ELGs we consider only the galaxies from the complete sample derived in section § 2, namely the galaxies that have $m_{L+C} \leq 12.0$ ($F_{L+C} \geq 6.7 \times 10^{-14}$erg sec^{-1} cm^{-2}).

It is worth stressing that within the range of our surveyed regions we deal with a field sample. No rich Abell cluster is present, only some Zwicky clusters. In Region 3, the Coma Cluster neighbours the southern border of our region (see Fig. 3 a), with its main body outside. This implies that any differences that we could find will not be due to the fact that the emission-line galaxies have the tendency to avoid rich clusters.

We first applied a Kolmogorov-Smirnov test to the redshift distributions of the two samples out to a velocity of 10000 km/s. Since the velocity distribution of the ZCAT falls off rapidly beyond 10000 km/s, we limited our statistic to a subsample with velocities below this value. The comparison distribution was constructed by selecting at random from the ZCAT the same number of objects (N) and in the same volume of space as in the ELG sample. This randomly generated distribution was computed for 1000 samples of N ZCAT galaxies, and the results averaged to produce the final comparison. The results indicate that the two samples are drawn from the same parent population (KS=0.55).

To better address the question of whether or not the two samples have the same spatial distributions, we used a nearest neighbour (NN) test (Thompson 1983). The cone-diagrams give also an impression of the overall spatial structures, but as the

Table 3. The main characteristics of the void galaxies.

name	v	D_{NN} (HS-ZCAT)	D_{NN} (HS-HS-ZCAT)	D_{NN} (HS-ZCAT(late))	B	M	Flux [OIII] λ5007	EW [OIII] λ5007
	km/s	h^{-1} Mpc	h^{-1} Mpc	h^{-1} Mpc			erg sec^{-1} cm^{-2}	Å
(1)	(2)	(3)	(4)	(5)	(6)	(7)	(8)	(9)
HS1342+3354	1692.5	1.93	1.77	2.50	19.2	-12.73	1.85e-14	-271.49
HS1349+3942	1695.5	2.20	1.77	2.20	16.7	-15.20	3.07e-14	-46.69
HS1236+3821	2214.8	3.85	3.85	3.85	15.3	-17.25	3.38e-14	-23.80
HS1226+3719	3306.0	6.63	-	-	19.2	-14.24	0	0
HS1236+3937	5571.4	8.68	7.88	8.68	18.7	-15.88	2.54e-14	-466.52
HS1232+3947	6355.6	5.26	3.97	5.26	17.2	-17.67	3.80e-14	-130.20
HS1240+3721	6582.3	3.34	3.34	3.34	17.9	-17.05	0	0
HS1332+3426	6664.5	4.45	2.06	4.45	18.6	-16.37	1.97e-14	-162.54
HS1328+3424	6849.1	2.76	2.06	2.76	16.8	-18.23	9.36e-15	-17.90
HS1310+3801	6954.1	3.43	3.43	3.43	18.1	-16.97	-	-
HS1529+4512	7088.0	6.83	4.45	10.20	17.9	-17.22	1.49e-14	-94.35
HS1325+3255	7942.5	3.46	3.46	3.46	19.2	-16.16	2.39e-14	-388.33
HS1306+3320	8131.0	3.45	3.45	3.58	16.9	-18.51	4.04e-14	-108.82
HS1526+4045	8777.3	3.59	3.59	3.59	17.0	-18.60	5.40e-15	-10.91
HS1341+3117	8846.4	5.69	5.69	5.69	18.6	-17.00	1.68e-14	-80.30
HS1429+4511	9742.1	11.39	8.43	11.39	18.0	-17.81	2.45e-15	-7.89
HS1507+3743	9776.2	5.27	5.27	8.21	17.9	-17.93	2.19e-13	-1465.93

plots are only two dimensional representations, the projection effects could affect some of the results. The nearest neighbour test calculates the real separation in the 3-dimensional space and also quantifies the results. Eder et al. (1989) showed that this test is particularly sensitive to the lack of clustering in a sample, and is therefore recommended for field samples. We limited again our statistic to subsamples with velocities less than 10000 km/s. We have computed two distributions. One gives the separation between each ELG galaxy of the sample (N objects) and the nearest ZCAT galaxy in the same field, but taken into consideration the edge effects. This means that the ZCAT galaxies were taken from a slightly larger field than that of the ELGs. For the second distribution we followed the same procedure as for the redshift distribution: a randomly selected sample of N galaxies was taken from the ZCAT catalogue. We calculated then the separation between each of the N ZCAT galaxies and its nearest ZCAT neighbour, again with edge effects considered.

The NN distributions are shown in Fig. 5. The overall impression is that the two distributions are quite similar. There seems to be an excess of ELGs at intermediate separations, around 2 h^{-1}Mpc, but the errors in each bin are quite big, due to the pure number statistics. There are also some ELGs at higher separations, where the ZCAT do not contribute. But these differences cannot change the overall similarity between the two distributions. This is confirmed by a Kolmogorov-Smirnov test which gives a KS=0.59, which means that the two distributions are identical. We should notice that some of the very isolated galaxies are not contained in the complete sample and therefore were not included in the computation of the NN test. These galaxies produce a tail of high separations in the distribution of ELGs, which sharpen the difference between the two distributions and make the ELGs to be more uniformly distributed than the giant galaxies.

The results of our statistical tests should be considered with caution, since the comparison ZCAT is not complete up to 15.5. The incompleteness of the comparison catalogue could introduce some errors that cannot be controlled. Unfortunatelly, until the pulic release of the CfA2, the ZCAT is the only catalogue that samples the distribution of the normal galaxies on a large enough extent.

3.4. Discussion

In this section we discuss the significance of our findings in some of the nearby voids. We refer only to the two nearest and best defined voids presented in Figure 2a, Void 1 and Void 2. First we estimate how many normal galaxies brighter than 15.5 we expect to find in the voids if the galaxies would be uniformly distributed. We consider the ZCAT galaxies brighter than 15.5 because the voids were defined by the distribution of these galaxies. We calculate the volume of Void 1 considering for simplicity an elipsoid shape with the diameters of the main axis: 3500 km/s, 1^h30^m and 15° (in radial velocity, Righ Ascension and Declination). We took also into consideration that not all the volume of the void was surveyed. At a distance of z=0.01 this will give a volume of 1289 h^{-3}Mpc^3. If we integrate the luminosity function derived by de Lapparent et al. (1989), over the magnitude range that includes galaxies brighter than 15.5, one would expect to find 106 galaxies brighter than 15.5. This result is obtained on the assumption that the galaxies were independently and randomly distributed, which is obviously not the case. One could of course correct for the fraction of galaxies that are not independent by using the autocorrelation function.

Table 4. Void galaxies in the ZCAT sample fainter than B=15.0.

	ZCAT name	other name	v (km/s)	B	T
Void 1	1149+3510	MK641	2165	16.5	
	1240+3541	-	1806	17.0	
Void 2	1227+3311	CG1027	5606	15.7	
	1230+3952	PGC41579	6212	16.0	Sc
	1305+3307	PGC45451	5300	16.0	Sd
	1305+3302	PGC45481	6753	16.0	Sd

For simplicity we consider only our rough estimates and we obtained an underdensity of 106. For Void 2 we obtain a volume of $1793\,h^{-3}Mpc^3$ and an underdensity of 57. This is the underdensity in the distribution of the normal galaxies.

The number of ELG one would expect in the voids was calculated using the space densities derived in subsection § 3.1, $\Phi = 0.011\,Mpc^{-3}$. We then estimate to find 44 ELGs in Void 1 and 47 ELGs in Void 2. This would be the case if our sample would be 100% complete over the magnitude range for which the space densities were considered. We already mentioned that the incompleteness factor was 2.04, therefore we should expect only 22 galaxies in Void 1 and 23 galaxies in Void 2. We found one ELG in Void 1 (a second one is not an ELG, see § 4) and 7 ELGs in Void 2 (of which 2 are at the rim of the void), which means we did not find a significant void population at the density that was tested (the density of the walls and filaments). Then the void population has either a density that is at least a factor 4.5 lower, or alternatively, that the void population is even fainter than the limits of our survey, and we reached only the brightest peaks of such population. One cannot reject the hypothesis that the few galaxies found in voids do not form a population, rather they represent fluctuations of the large scale structure. This would explain why some voids were found to contain a few galaxies and other voids to be empty (Rosenberg et al. 1994, Pustil'nik et al. 1995).

4. The properties of the void galaxies

A natural question that would arise from a study that has the goal to search for galaxies in voids is whether the galaxies found in the low density regions have special properties in comparison with the characteristics of the total sample. We did not find a real void population, but we could still comment on the properties of the isolated galaxies found in some voids. Table 3 gives the main parameters of the void galaxies from the surveyed region analysed in this paper. The galaxies are ordered with respect of increasing the radial velocity, because the isolation of the galaxies also increases with distance. Column (1) contains the name of the galaxies and Column (2) gives the radial velocity. In the following columns we listed the separation between our galaxies and their nearest bright ZCAT neighbour, D_{NN}(HS-ZCAT) (Column (3)); between our galaxies and their nearest neighbour, D_{NN}(HS-HS-ZCAT) (which can be also one galaxy from our sample or a bright ZCAT) (Column (4)) and between our galaxies and their nearest late-type bright ZCAT neighbour, D_{NN}(HS-ZCAT(late)) (Column (5)). For one galaxy, HS1226+3719, which is a galaxy with absorption (see discussion below), only the separation to its nearest bright ZCAT is given. Then we give the apparent B magnitudes (Column (6)), the absolute M_B magnitude (Column (7)), the flux of the [OIII] λ5007 line (Column (8)) and the EW of the same line (Column (9)). For the galaxies for which the [OIII] λ5007 line is not detected, the fluxes and EW are set to 0. For one galaxy, HS1310+3801, the fluxes and EW are not available. This galaxy was already known in the literature and it was not observed by us, and therefore was also not included in the statistical analyse.

The separations of the void galaxies show that 50% have the nearest neighbour among themself. This would suggest that the void galaxies are not uniformly distributed but also have the tendency to form fainter structures inside the bigger voids. Unfortunately, the low number of our isolated galaxies cannot allow us to draw any definitive conclusion. Nevertheless, some fainter ZCAT galaxies have been found to associate with some of our void galaxies. For example the Arch is followed by four faint ZCAT galaxies, and from these, all are late types. In Table 4 we list the ZCAT galaxies we found in Voids 1 and 2, respectively (even though they do not come from the complete sample), together with their main parameters (velocity, B magnitude and T morphological type, when available). The Arch seems also to divide Void 2 in three smaller voids. Lindner et al. (1996) and Szomoru et al. (1996b) also suggested that the galaxies found in voids have the tendency to cluster. In addition, 75% of our void galaxies have the nearest ZCAT neighbour among the late type galaxies. This should not come as a surprise since the late type galaxies have the tendency to be less clustered than the early types, which would preferentially form the skeleton of the clusters.

The absolute magnitudes of our void galaxies range between $-12.7 < M_B < -18.5$ which means that all of them are dwarfs. These galaxies are therefore intrinsically faint objects, quite different from the galaxies that were found in the Bootes void (Weistrop et al. 1995), which were mainly M^* galaxies or brighter. Nevertheless, the distribution of absolute magnitudes of our parent sample starts to drop around $M_B = -17$ and only a few galaxies are found in the range $-12 < M_B < -15$. If a faint void population had typical luminosities around $M_B = -15$ and below, we would just start to detect it, since we are very incomplete at the faint end. The few galaxies we found in the voids could constitute the tip of the iceberg of the void population.

The spectroscopic properties of our void galaxies are very different and they do not belong to only one class of objects. The EW and fluxes encompass mostly the whole range of values from the parent sample. Some void galaxies have extremely large EW and fluxes of the [OIII] λ5007 line whether others are barely detectable. In Figure 6 we give some example of void galaxy spectra. The plots show that the galaxies we found in voids have different degrees of ionization, from very high ionization objects with very faint continuum, close to the extreme case of Searle-Sargent objects, up to very low ionization galaxies and strong continuum which indicate an underlying older

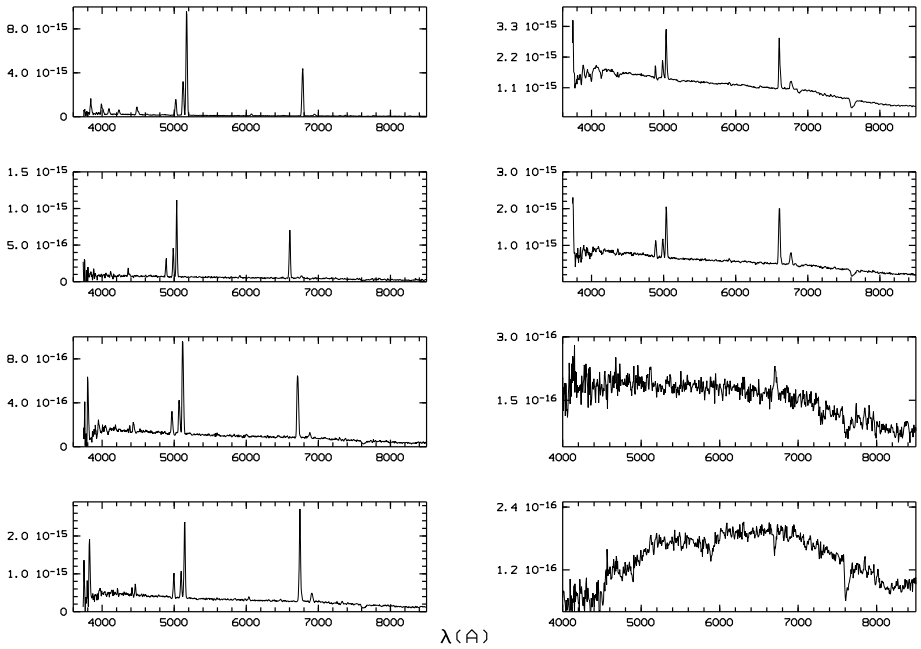

Fig. 6. Spectra of void galaxies. The y-axes contain the fluxes per unit of wavelength, F_λ (erg sec^{-1} cm^{-2} Å^{-1}) while the x-axes contain the wavelength, λ (Å).

stellar population. Amazingly, we found also one object that has no detectable [OIII] λ5007 line; the only emission-line being Hα. This object was selected mainly because of the blue continuum and was considered a second priority candidate (see Paper 1 for a detailed description of the selection procedure) and was not included in the statistical analyse. But the most unexpected void galaxy is HS1226+3719, an object that entered in our sample as a failure of our selection procedure, being a galaxy with absorption. On the other hand this galaxy is one of our best void candidates, with an isolation of $D_{NN} = 6.63h^{-1}$Mpc, and lying in the centre of Void 1. (Figure 2 a). This result fact makes us wonder whether a population of dwarf elliptical galaxies would not be in fact the hidden void population which would recover the biasing theories. But it is known (Binggeli 1989) that the dwarf ellipticals are the most clustered galaxies in the Universe, which populate mainly the clusters. This still do not exclude the possibility that the voids would be occupied by a population of dwarf red galaxies similar to the dwarf ellipticals we see now in clusters.

5. Summary and conclusions

Our present study did not find the voids occupied by a homogenous population of dwarf galaxies. We found a few galaxies in the very well defined nearby voids, but the number of void galaxies is not significant at the density level of field galaxies. We could interpret this result in the sense that a void population, if any, should have the density at least a factor 4.5 lower than the density of walls and filaments. Another possibility is that we start to see the brightest peaks of such population and we are still not faint enough to really sample these objects. Alternatively, there is no void population, and the galaxies we found in voids were only fluctuations from the normal distribution. This would explain why some voids were found to be empty and other to contain a few galaxies. On the other hand we should also remember that we were probing the voids only with emission-line galaxies, and from these, we are mainly sensitive in the high ionization objects. We are complete in the galaxies with large equivalent widths and we start to miss objects that have fainter EW. These objects are mainly low ionization and are better detected by Hα surveys, like the surveys based on objective prism IIIaF plates (UCM survey, Zamorano et al. (1994)). Therefore the voids were still not probed by low ionization emission-line objects. Nevertheless the UCM galaxies seem also to follow the same structures as the normal galaxies (Gallego 1995), but the UCM sample do not contain galaxies as faint as we detect. We should also keep in mind that the IIIaJ selected emission-line galaxies contribute only 7% from the total number of galaxies (Salzer 1989). It was suggested that the small HII galaxies are the best candidates to fill the voids, but it could still be that a population of old red dwarf galaxies would fill the voids. These galaxies do not have a strong spectroscopic signature like an emission spectrum and they are gas poor and therefore are not detected by HI surveys. If they were fainter than M_B=-15, they would be not properly sampled by any survey that search them on direct images.

Coming back to our ELGs we suggest that the few galaxies that we found in voids have also a tendency for clustering. This result is far from being secure, but some of our void galaxies seem to associate with faint late-type ZCAT galaxies. For example our Arch of 7 ELGs in Void 2 is followed by four faint ZCAT galaxies. The Arch seem to divide that bigger void in 3 smaller voids. And not at the end, 75% from our isolated galaxies have their nearest neighbours among themself. These results are close to some results of N-body simulations (Dubinski et al. 1993, van de Weygaert & van Kampten 1993) or with the ob-

servational results of an HI survey in the Bootes void (Szomoru 1996). It was thus suggested that smaller scale voids disappear within larger voids but the frozen-in remnants of small walls would produce smaller substructures inside the larger voids. Lindner et al. (1996) also suggest a hierarchical distribution of galaxies and voids, in the sense that superclusters and clusters delimit bigger voids, bright galaxies some smaller voids and faint galaxies delimit very small voids, inside the bigger ones.

Overall the main characteristics of the ELG spatial distributions are:

1. The ELGs are better than normal galaxies for tracing the luminous matter at further distance;

2. The ELGs have a small tendency to be more evenly distributed than the ZCAT galaxies, with some galaxies lying in some voids or at the rim of the voids.

3. A filamentary structure (the Arch), populated only by faint ELGs, has been found to cross a big void in front of the Great Wall.

4. The void galaxies are intrinsically faint and they do not have special spectroscopic properties in comparison with the other ELGs in the field.

Acknowledgements. We would like to thank Dr. A.P. Fairall for the careful review of this manuscript and to Dr. H. Hagen for his contribution during the work with the HS data base. We also thank Dr. S. Pustil'nik for providing us some unpublished data on Markarian galaxies. We gratefully acknowledge the comments and discussions with Drs. B. Binggeli, A. Burkert, R. P Kirshner, D. Thompson, D. Valls-Gebaud. We would also like to thank the Calar Alto staff for their support during the observations. U. Hopp acknowledge the support by the SFB 375 by the Deutsche Forschungsgemeinschaft.

References

Binggeli, B. 1989, in "Large Scale Structure and Motions in the Universe ", p. 47, eds. Mezzetti et al.
Binggeli, B., Tarenghi, M., Sandage, A. 1990, A&A 228, 42
Bothun , G.D., Beers, T.C., Mould, J.R., Huchra, J.P. 1986, ApJ 308, 510
Dekel, A., Silk, J. 1986, ApJ 303, 39
de Lapparent, V., Geller, M.J., Huchra, J.P. 1989, ApJ 343, 1
Dey, A., Strauss, M.A., Huchra, J.P. 1990, AJ 99, 463
Dubinski, J., da Costa, L.N., Goldwirth,, D.S., Piran, T. 1993, ApJ 410, 458
Eder J.A., Schombert J.M., Dekel A., Oemler A. 1989, ApJ 340, 29
Gallego, J. 1995, PhD thesis (Madrid)
Hagen, H.-J., Groote, D., Engels, D., Reimers, D. 1995, A&AS 111, 195
Hopp, U. 1994, in: ESO/OHP Workshop "Dwarf Galaxies", ESO Conference and Workshop Proceedings No. 49, p. 37, ed. G. Meylan and P. Prugniel
Hopp, U., Kuhn, B., Thiele, U., Birkle, K., Elsässer H. 1995, A&AS 109, 537
Huchra, J. Geller, M., Clemens, C., Tokarz, S., Michel, A. 1992, Bull. C.D.S. 41, 31
Huchra, J., Geller, M.J., Clemens, C.M., Tokarz, S.P., Michel, A. 1995, The Center for Astrophysics Redshift Catalogue, electronic version
Kirshner, R.P., Oemler, A., Schechter, P.L., Shectman, S.A. 1981, ApJ 248, L57
Kirshner, R.P., Oemler, A., Schechter, P.L., Schectman, S.A. 1983a, in IAU Symposium 104, Early Evolution of the Universe and Its Present Structure, ed. G.O. Abell and G. Chincarini (Dordrecht:Reidel), p. 197
Kirshner, R.P., Oemler, A., Schechter, P.L., Schectman, S.A 1983b, AJ 88, 1285
Kuhn, B., Hopp, U., Elsässer, H. 1997, A&A 318, 405
Lindner, U., Einasto, M., Einasto, J., Freudling, W., Fricke, K., Lipovetsky, V., Pustilnik, S., Izotov, Y., Richter, G. 1996, A&A 314, 1
Moody, J.W., Kirshner, R.P., MacAlpine, G.M., Gregory, S.A. 1987, ApJ 314, L33
Popescu, C.C. 1996, Ph.D thesis, Heidelberg
Popescu, C.C., Hopp, U., Elsässer, H., Hagen, H. 1995, in: Proceedings of the XXXth Rencontre de Moriond Series: Clustering in the Universe, eds. S. Maurogordato, C. Balkowski, C. Tao, J. Trân Thanh Vân. p. 77
Popescu, C.C., Hopp, U., Hagen, H., Elsässer H. 1996, (Paper 1) A&AS 116, 43
Pustil'nik, S.A., Ugryumov, A.V., Lipovetsky, V.A., Thuan, T.X., Guseva, N.G. 1995, ApJ 443, 499
Rosenberg, J.L., Salzer, J., Moody, J.W., 1994, AJ 108, 1557
Salzer J.J. 1989, ApJ 347, 152
Salzer J.J., Hanson, M.M., Gavazzi G. 1990, ApJ 353, 39
Sandage, A. 1975, Galaxies and the Universe, University of Chicago press
Sanduleak, N. Pesch, P. 1982, ApJ 258, L11
Schmidt, M 1968, ApJ 151, 393
Szomoru, A., van Gorkom, J.H., Gregg, M.D 1996a, AJ 111,
Szomoru, A., van Gorkom, J.H., Gregg, M.D., Strauss, M.A. 1996b, AJ 111, 2150
Tifft, W.G., Kirschner, R.P., Gregory, S.A., Moody, J.W. 1986, ApJ 310, 75
Thompson, L.A. 1983, ApJ, 266, 446
Thuan, T.X., Gott, J.R., Schneider, S.E., 1987, ApJ, 315, L93
Thuan, T.X., Alimi, J-M, Gott, J.R., Schneider, S.E. 1991, ApJ 370, 25
van de Weygaert, R., van Kampen, E. 1993, MNRAS 263, 481
Weinberg, D.H., Szomoru, A., Guhathakurta, P., van Gorkom, J.H., 1991, ApJ 372, L13
Weistrop D. 1989, AJ 97, 357
Weistrop D., Downs R.A. 1988, ApJ 331, 172
Weistrop, D., Hintzen, P., Liu, C., Lowenthal, J., Cheng, K,-P., Oliversen, R., Brown, L., Woodgate, B. 1995, AJ 109, 981
Zamorano, J., Rego, M., Gallego, J., Vitores, A.G., González-Riestra , R., Rodíguez-Caderot, G. 1994, ApJS 95, 387

This article was processed by the author using Springer-Verlag LaTeX A&A style file *L-AA* version 3.